

# Alcohol Amination with Ammonia Catalyzed by an Acridine-Based Ruthenium Pincer Complex: A Mechanistic Study

Xuan Ye,<sup>†</sup> Philipp N. Plessow,<sup>†,‡</sup> Marion K. Brinks,<sup>§</sup> Mathias Schelwies,<sup>§</sup> Thomas Schaub,<sup>§</sup> Frank Rominger,<sup>||</sup> Rocco Paciello,<sup>§</sup> Michael Limbach,<sup>†,§</sup> and Peter Hofmann<sup>\*,†,||</sup>

<sup>†</sup>Catalysis Research Laboratory (CaRLa), Im Neuenheimer Feld 584, D-69120 Heidelberg, Germany

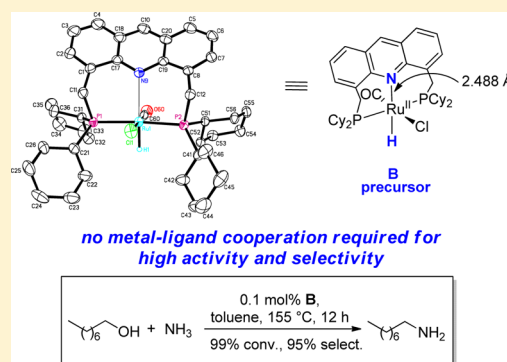
<sup>‡</sup>Quantum Chemistry, BASF SE, Carl-Bosch-Straße 38, D-67056 Ludwigshafen, Germany

<sup>§</sup>Synthesis & Homogeneous Catalysis, BASF SE, Carl-Bosch-Straße 38, D-67056 Ludwigshafen, Germany

<sup>||</sup>Organisch-Chemisches Institut, Ruprecht-Karls-Universität Heidelberg, Im Neuenheimer Feld 270, D-69120 Heidelberg, Germany

## Supporting Information

**ABSTRACT:** The mechanistic course of the amination of alcohols with ammonia catalyzed by a structurally modified congener of Milstein's well-defined acridine-based PNP-pincer Ru complex has been investigated both experimentally and by DFT calculations. Several key Ru intermediates have been isolated and characterized. The detailed analysis of a series of possible catalytic pathways (e.g., with and without metal–ligand cooperation, inner- and outer-sphere mechanisms) leads us to conclude that the most favorable pathway for this catalyst does not require metal–ligand cooperation.



## INTRODUCTION

The direct synthesis of amines from alcohols via a hydrogen-borrowing mechanism is atom-economical and environmentally benign, with water as the only stoichiometric side product. The commonly accepted mechanistic pathway is a sequence of alcohol oxidation, aldehyde amine condensation, and imine reduction (Figure 1).<sup>1</sup>

A variety of transition-metal-based homogeneous catalysts (e.g., based on Ru,<sup>2</sup> Ir,<sup>3</sup> Cu,<sup>4</sup> Fe,<sup>5</sup> and Pd<sup>6</sup>) have been developed for this reaction, and they even outperform some of the state-of-the-art heterogeneous catalysts for alcohol amination with NH<sub>3</sub><sup>7</sup> with respect to substrate scope, selectivity, and activity.<sup>1a,8</sup> Among those, Ru-based metal precursor/ligand combinations C and D (Figure 1)<sup>9</sup> and especially Milstein's well-defined acridine-based PNP-pincer Ru complex A<sup>9a</sup> are powerful catalysts with unprecedented reactivity and selectivity for primary amines employing ammonia as the nitrogen source.

This exceptional performance of A has been attributed to the acridine-based PNP-pincer ligand framework, which cooperates with the metal via dearomatization of the acridine backbone,<sup>10</sup> as demonstrated by Milstein and co-workers in stoichiometric studies of A with H<sub>2</sub> and NH<sub>3</sub>.<sup>11,12</sup> This reversible aromatization–dearomatization is also considered a pivotal mechanistic feature for a broader range of pyridine-based pincer complexes<sup>13,14</sup> in numerous catalytic transformations other than alcohol amination,<sup>9a</sup> including hydrogenation of carbonates, dehydrogenative homocoupling of alcohols or alcohols and amines, and even water splitting.<sup>15,16</sup> Nevertheless, detailed

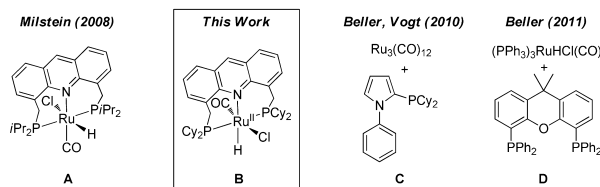
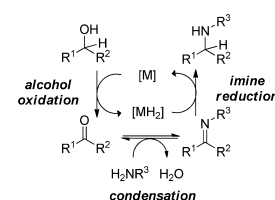


**Figure 1.** Ruthenium-based homogeneous catalysts or catalyst systems A–D for the amination of alcohols with NH<sub>3</sub> (bottom) and the basic mechanistic pathway (top).

mechanistic studies of acridine-based systems are scarce,<sup>11</sup> and the impact of the pincer ligand framework on the selectivity toward primary amines remains speculative. The present study aims to address those open questions.

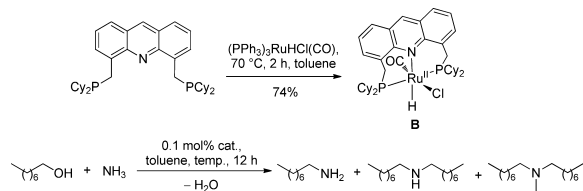
Received: September 13, 2013

Published: March 31, 2014

## RESULTS AND DISCUSSION

**Experimental Investigation.** In analogy to a synthetic procedure described by Milstein and co-workers,<sup>9a</sup> we synthesized the new complex **B** with cyclohexyl substituents on the P atoms in 74% isolated yield from  $(\text{PPh}_3)_3\text{Ru}(\text{H})(\text{Cl})(\text{CO})$  and 4,5-bis(dicyclohexylphosphinomethyl)acridine<sup>9a</sup> (70 °C, 2 h; cf. the reaction shown at the top of Table 1). In a

**Table 1. Synthesis of Acridine-Based Ru Pincer Complex B and Tests of Catalysts A–D in the Amination of 1-Octanol with  $\text{NH}_3$ <sup>a</sup>**



entry	cat.	T (°C)	conv. (%) <sup>a</sup>	sel. (%) <sup>b</sup>
1	A	135	37	85
2	A	155	99	95
3	B	135	73	91
4	B	155	99	95
5	C	155	20	32
6	D	155	16	69

<sup>a</sup>[1-octanol] = 1 M, 0.1 mol % catalyst,  $p(\text{NH}_3)$  = 35–40 bar, toluene (50 mL), 12 h, 160 mL stainless-steel autoclave. <sup>b</sup>Selectivity in 1-octylamine.

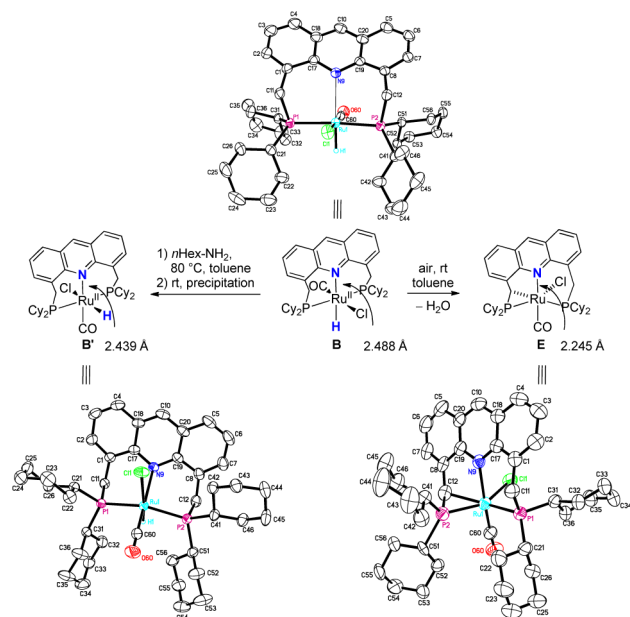
benchmark reaction, namely, the amination of 1-octanol with  $\text{NH}_3$ , the modified catalyst **B** exhibited reactivity and selectivity comparable to those of Milstein's prototype **A** and superior to those of the other Ru-based two-component catalysts **C** and **D** (Table 1).<sup>9</sup>

Red crystals of **B** were obtained from a toluene/hexane mixture, and its molecular structure in the crystal revealed a pseudo-octahedral geometry of the Ru center with an elongated Ru–N bond in comparison with **A**<sup>16</sup> (2.488 vs 2.479 Å; cf. Scheme 1). Noteworthy is the trans geometry of the acridyl N and the hydride ligand, which contrasts the cis geometry reported by Milstein and co-workers in their system.<sup>16</sup> Interestingly, crystals of complex **B'**, a stereoisomer of complex **B** that features the cis geometry of the acridyl N and the hydride ligand as reported for **A**, were obtained upon cooling of a toluene solution of **B** and 1-hexylamine that had been heated at 80 °C for 16 h (Ru–N = 2.439 Å; Scheme 1).

When the recrystallization of **B** was carried out under air, black/brown crystals of the new complex **E** were obtained, and its crystal structure revealed that one of the benzylic C–H units was cyclometalated by the Ru center. In comparison to the non-cyclometalated complexes **B** and **B'**, the Ru–N bond distance was significantly shortened (2.245 Å; cf. Scheme 1). This cyclometalation reaction under mild oxidative conditions implies that the benzylic protons of the PNP-pincer ligands are susceptible to C–H activation by the Ru center.

The stoichiometric reaction of **B** with a primary alcohol (e.g., benzyl alcohol, 1-octanol, each 2–4 equiv) without an external base did not yield alcohol oxidation products according to NMR analysis (toluene-*d*<sub>8</sub>, 70 °C, 16 h). In the presence of NaOtBu or NaH (4–14 equiv), benzyl benzoate, the product of a formal Claisen–Tishchenko reaction, was obtained within

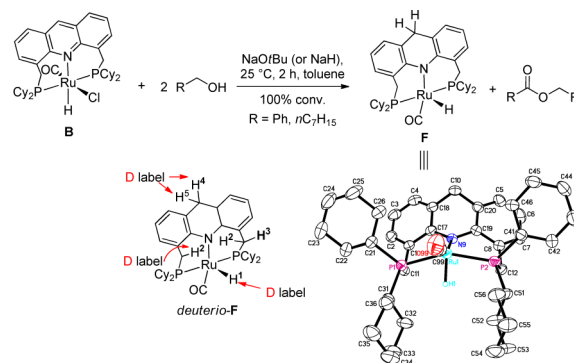
**Scheme 1. Solid-State (X-ray) Molecular Structures of Catalyst Precursor B, Its Isomer B', and Complex E<sup>a</sup>**



<sup>a</sup>Ellipsoids are drawn at 50% probability, and H atoms have been omitted for clarity. **B**: P–Ru–N, 91.92(5)/92.08(5)°; H–Ru–P1, 88.9(11)°; H–Ru–N, 173.9(11)°; Ru–CO, 1.801(3) Å; Ru–P, 2.316(8)/2.3073(8) Å; Ru–N, 2.488(2) Å; Ru–Cl, 2.4792(8) Å; Ru–H, 1.45(3) Å. **B'**: P–Ru–N, 90.73(4)/89.66(4)°; H–Ru–Cl, 172.3(7)°; OC–Ru–P1, 92.34(7)°; Ru–CO, 1.796(2) Å; Ru–P, 2.3145(5)/2.3264(6) Å; Ru–N, 2.4389(17) Å; Ru–Cl, 2.5195(6) Å; Ru–H, 1.507(19) Å. **E**: P2–Ru–N, 87.11(12)°; P2–Ru–Cl, 145.25(6)°; N–Ru–Cl, 83.91(11)°; P–Ru–P, 114.32(6)°; Ru–CO, 1.805(7) Å; Ru–P, 2.3121(15)/2.2466(16) Å; Ru–N, 2.249(4) Å; Ru–Cl, 2.4609(15) Å; Ru–C, 2.208(5) Å.

only 2 h at room temperature. Concurrently, the new Ru complex **F** with a dearomatized acridine backbone formed from **B** in a clean reaction (Scheme 2).<sup>17</sup> The crystal structure of **F** revealed that the Ru sits in the center of a pseudotrigonal bipyramid and that the central ring of the dearomatized acridine ligand adopts a boat-shaped structure. The Ru–N

**Scheme 2. Stoichiometric Alcohol Oxidation by Catalyst Precursor B in the Presence of Base and Solid-State (X-ray) Molecular Structure of F<sup>a</sup>**

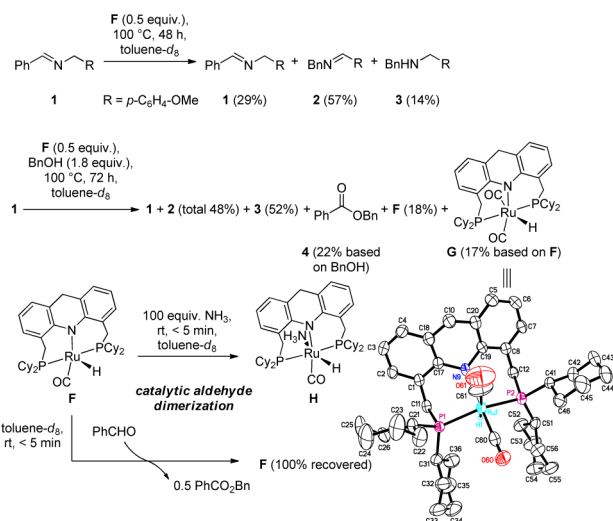


<sup>a</sup>Ellipsoids are drawn at 50% probability, and H atoms have been omitted for clarity. **F**: P–Ru–N, 91.38(8)/91.40(8)°; N–Ru–CO, 153.29(14)°; P–Ru–P, 155.02(3)°; Ru–CO, 1.814(4) Å; Ru–P, 2.3196(10)/2.3219(9) Å; Ru–N, 2.109(3) Å; Ru–H, 1.49(4) Å.

bond is significantly shortened in comparison with that in **B** (2.109 vs 2.488 Å) upon dearomatization and is in the range of the Ru–N bond in the *i*Pr derivative observed by Milstein (2.109 vs 2.171 Å).<sup>11</sup> With the deuterated substrate benzyl alcohol- $\alpha,\alpha\text{-d}_2$ , deuterium scrambling into the hydride (H<sup>1</sup>), benzylic C–H (H<sup>2</sup>), and methylene C–H (H<sup>4</sup>, H<sup>5</sup>) positions of **F** was observed, even at room temperature (Scheme 2).<sup>18</sup> Scrambling including the phosphine substituents has also been observed previously in the reaction of **A** with D<sub>2</sub> and KOH.<sup>11</sup>

Heating a mixture of **F** (0.5 equiv) and imine **1** to 100 °C for 2 days predominantly isomerized the imine's double bond. Only minor amounts of benzylamine (**3**) were formed, as shown by <sup>1</sup>H NMR analysis (1:2:3 = 29:57:14; Scheme 3). The

### Scheme 3. Intermediate **F** as a Reductant<sup>a</sup>

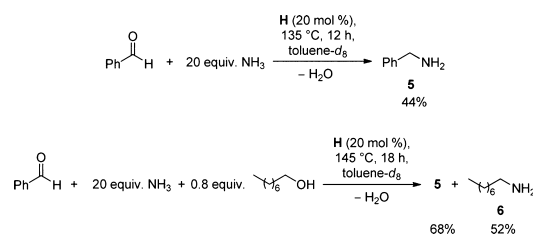


<sup>a</sup>R = *p*-OMe-C<sub>6</sub>H<sub>4</sub>, Ph = phenyl, Bn = benzyl. **G**: P–Ru–N, 88.74(8)/89.29(8)°; H–Ru–P1, 72.5(16)°; H–Ru–N, 89.6(16)°; Ru–CO, 1.835(5)/1.945(7) Å; Ru–P, 2.3254(11)/2.3380(11) Å; Ru–N, 2.238(3) Å; Ru–H, 1.34(4) Å.

conversion of **F** was high (70%), but its further fate remained unclear. When the same reaction was repeated in the presence of benzyl alcohol (1.8 equiv), the yield of **3** increased significantly within 3 days (52 vs 14%). Benzyl benzoate (**4**) was the final organic oxidation product, and it was formed in 22% yield (based on benzyl alcohol). Besides unreacted **F** (18% yield), the bis(carbonyl) Ru hydride complex **G** (17% yield based on **F**) was observed in the product mixture.<sup>19</sup> The second CO ligand might originate from decarbonylation of benzyl alcohol.<sup>20</sup> The sum of complexes **F** and **G** in the final solution accounted for ca. 35% of the total amount of added Ru, indicating the above-mentioned decomposition of **F**. Thus, **F** can serve as a reductant in the transformation of an imine to an amine.

Both benzaldehyde and NH<sub>3</sub> already reacted with **F** at room temperature, leading to either the rapid disproportionation of benzaldehyde to give **4** or the rapid coordination of NH<sub>3</sub> to the Ru center to afford **H** (Scheme 3).<sup>21</sup> Heating a mixture of benzaldehyde, complex **H** (0.2 equiv), and NH<sub>3</sub> (20 equiv) at 135 °C for 12 h resulted in the formation of benzylamine (by <sup>1</sup>H NMR analysis) along with multiple organic side products (e.g., benzonitrile, benzamide, benzyl benzoate, and *N*-benzylidene-1-phenylmethanamine; cf. Scheme 4). The majority of **H** (80%) decomposed to give a mixture of unidentified

### Scheme 4. Reaction of Alcohol/Ammonia and Aldehyde under the Influence of Complex **H**



Ru species. The yield of benzylamine exceeded the maximum yield possible for a stoichiometric reductive amination by a factor of 2, which points to a catalytic reaction. The reductants in this stoichiometric redox transformation are proposed to be **H** and the in situ-generated benzylidene imine, which is oxidized to PhCN. The same reaction, but now in the presence of 1-octanol (0.8 equiv), gave benzylamine and octylamine in greater than stoichiometric yield (68 and 52%, respectively; cf. Scheme 4) in addition to multiple byproducts (i.e., heptyl nitrile, octyl benzoate, *N*-benzylidene-1-phenylmethanamine, *N*-benzylidene-1-heptylmethanamine). The higher yield of **5** (44 vs 68%) implies that the alcohol facilitates the reductive amination of aldehyde by **H**.

When **B** (20 mol %) was heated in a mixture of 1-octanol and NH<sub>3</sub> (6 equiv) at 150 °C for 16 h, complex **H** was identified as the major organometallic species (30% by <sup>31</sup>P NMR spectroscopy) in addition to the expected amine/imine mixture. A series of control experiments was performed (0.1 mol % **B**, 135–140 °C, 12 h, toluene or THF, autoclave) to prove that primary and secondary amines do not interconvert under the given reaction conditions. Amination of 1-octanol with NH<sub>3</sub> (6 equiv) in the presence of 1-octylamine (1 equiv) yielded negligible amounts of dioctylamine, and only 50% of the initial 1-octanol was converted, indicating a moderate inhibitory effect of the amine product on the reaction rate. Amination of 1-octanol with NH<sub>3</sub> (12 equiv) in the presence of hexanal (1 equiv) gave a mixture of 1-octylamine and 1-hexylamine (39 and 19%, respectively) besides the corresponding nitriles. The reaction of solely 1-octylamine under our standard conditions afforded only traces of dioctylamine (~1%), and the same experiment with dioctylamine and NH<sub>3</sub> yielded only traces of 1-octylamine (<1%).

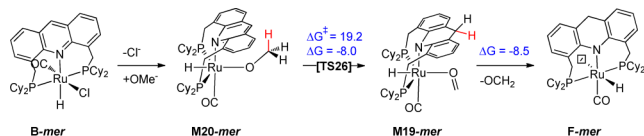
To summarize, catalyst precursor **B** readily oxidizes primary alcohols to esters in the presence of base at room temperature and is concurrently reduced to Ru hydride complex **F** featuring a dearomatized acridine pincer ligand. Complex **F** is capable of reducing imines to amines at elevated temperature, and reduction of imines by **F** is facilitated by the addition of an alcohol. In the presence of ammonia, complex **F** is rapidly converted to the NH<sub>3</sub>-coordinated Ru hydride complex **H** at room temperature. Complex **H** promotes the reductive amination of aldehydes with ammonia to generate primary amines, and catalytic turnover can be achieved at elevated temperature with both complex **H** and the in situ-generated imine (RCH<sub>2</sub>=NH) as sacrificial reducing agents. Complex **H** has also been characterized as the major Ru species in the reaction mixture of alcohol amination with ammonia catalyzed by precursor **B**. The primary amine selectivity in catalytic alcohol amination is sensitive to the ammonia pressure. The amine product from alcohol amination shows a moderate inhibitory effect on the turnover rate of this reaction. Lastly,

primary and secondary amines do not interconvert under the mentioned experimental conditions.

**Computational Investigation.** We carried out computational studies to rationalize these experimental findings. All of the geometries were optimized at the BP86/def2-SV(P)<sup>22</sup> level of density functional theory (DFT) with the corresponding effective core potential for ruthenium.<sup>23</sup> Calculations were carried out using the resolution-of-identity approximation and appropriate auxiliary basis functions<sup>24</sup> with TURBOMOLE.<sup>25</sup> Gas-phase free energies were obtained within the usual rigid-rotator, harmonic-oscillator approximation for 150 °C and 50 bar.<sup>26</sup> Absolute energies were obtained as single-point energies at the M06/def2-TZVP//BP86/def2-SV(P)<sup>27</sup> level of theory with GAMESS-US.<sup>28</sup> Solvent corrections to reaction free energies, obtained with COSMO-RS,<sup>29</sup> were typically <1.2 kcal/mol. Therefore, only gas-phase free-energies are discussed. The influence of solvation was investigated by computing solvation free energies at 150 °C and 50 bar with COSMO-RS using the parametrization for BP86/def-TZVP. Pure toluene and a toluene/methanol mixture with 90 mol % toluene were studied as solvents.

**Initiation.** Our proposed mechanism for dearomatization of **B** to give **F** in both the stoichiometric reaction with alkoxide and alcohol (Scheme 2) and catalytic alcohol amination is shown in Scheme 5. The alcohol is deprotonated by either the

#### Scheme 5. Proposed Mechanism for Initial Dearomatization of **B-mer** To Give **F-mer**<sup>a</sup>



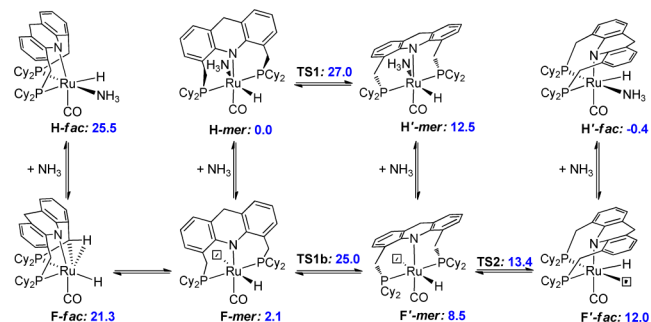
<sup>a</sup>Calculated free energies ( $\Delta G^\ddagger$ ,  $\Delta G$ ) are shown in kcal/mol.

alkoxide or ammonia. Dissociation of chloride and coordination of the alkoxide gives the complex **M20-mer**. Dearomatization can then occur by hydride transfer to the C9 position of the acridine ring, which requires only a relatively low barrier ( $\Delta G^\ddagger = 19.2$  kcal/mol).

Dearomatization induced by dihydrogen involving a direct hydride transfer from Ru to C9 was studied computationally by Milstein and co-workers.<sup>11</sup> As the computed barrier found in that work is significantly higher ( $\Delta G^\ddagger = 25.2$  kcal/mol), we think it is less relevant in this context. This is also in agreement with the difference in experimental conditions: Dearomatization with alkoxide/alcohol requires 2 h at 25 °C, while dearomatization with KOH/H<sub>2</sub> was reported after 48 h in refluxing toluene.<sup>11</sup>

**Impact of Stereoisomers and Imine Reduction by Complex **F**.** Formaldimine (CH<sub>2</sub>=NH) was used as the substrate in the computational investigations of the imine reduction step. We took into account different starting coordination geometries of the reductant **F**, inner-sphere versus outer-sphere mechanisms, and mechanisms with and without metal–ligand cooperation (for a detailed discussion, see the Supporting Information). As the dearomatized acridine-based PNP-pincer ligand can adapt both mer and fac coordination modes (Scheme 6),<sup>30</sup> four stereoisomers are possible for complex **F** (**F-fac**, **F-mer**, **F'-mer**, and **F'-fac**) and for the corresponding NH<sub>3</sub>-coordinated complex **H** (**H-fac**, **H-mer**, **H'-mer**, and **H'-fac**). Among those, **F-mer** turned out to be

#### Scheme 6. Stereoisomers of Pentacoordinate Ru–H Complex **F** and the Corresponding NH<sub>3</sub>-Coordinated Ru–H Complex **H** and the Isomerization Pathway<sup>a</sup>



<sup>a</sup>Calculated free energies ( $\Delta G^\ddagger$ ,  $\Delta G$ ) are shown in kcal/mol.

the most stable stereoisomer. **H-mer** was chosen as the reference point ( $G_{\text{H-mer}} = 0$  vs  $G_{\text{F-mer}} = 2.1$  kcal/mol).<sup>31,32</sup> The calculated structural features of **F-mer** correlate well with its experimentally obtained crystal structure (cf. Scheme 2).

The isomerization from **F-mer** to **F'-mer** involves flipping of the dearomatized acridine ring from one side of the PNP plane to the other, and the most favorable computed isomerization pathway consists of sequential NH<sub>3</sub> coordination to form **H-mer**, isomerization to give **H'-mer** via flipping of the ligand backbone, and NH<sub>3</sub> dissociation. The highest barrier in this stepwise isomerization arises from the change in the orientation of the dearomatized acridine backbone in **H-mer** ( $G_{\text{TS1}} = 27.0$  kcal/mol). Although the stereoisomers **F'-mer** and **F'-fac** are both higher in energy than **F-mer** ( $G_{\text{F'-mer}} = 8.5$  kcal/mol and  $G_{\text{F'-fac}} = 12.0$  kcal/mol vs  $G_{\text{F-mer}} = 2.1$  kcal/mol), they could be viable intermediates in the imine reduction step because of the high reaction temperature of 150 °C.

Mechanisms involving the fac geometry turned out to be the most favorable and will now be discussed in detail. Other investigated mechanisms and those involving the mer geometry can be found in the Supporting Information. The formation of Ru amide **M3'-fac** from **F'-fac** via the inner-sphere imine insertion was not only thermodynamically favored ( $\Delta G = -11.6$  kcal/mol; cf. Figure 2) but also had a low overall kinetic barrier (1.8 kcal/mol). The orientation of the dearomatized acridine central ring in Ru amide **M3'-fac** places the methylene

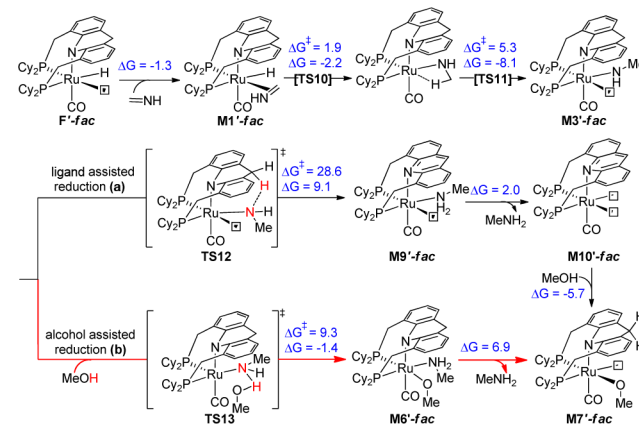
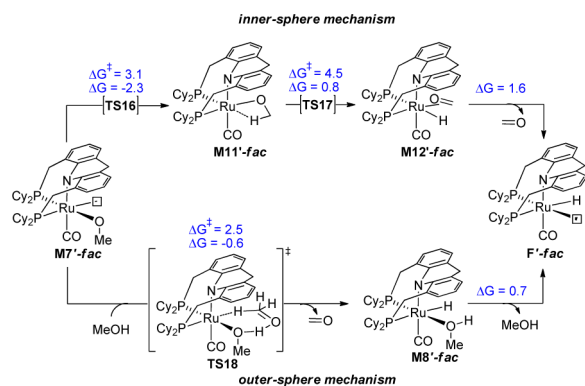


**Figure 2.** (a) Ligand-assisted reduction vs (b) inner-sphere alcohol-assisted reduction of methanimine by **F'-fac**. Calculated free energies ( $\Delta G^\ddagger$ ,  $\Delta G$ ) are shown in kcal/mol.

moiety in close proximity to the amide and renders metal–ligand cooperation with the dearomatized acridine ring by intramolecular protonation a reasonable pathway. However, the direct, intermolecular protonation of Ru amide  $M3'$ -*fac* by alcohol is energetically more favorable.<sup>33</sup> Rearomatization of the acridine backbone is therefore likely to occur only in the stoichiometric imine reduction that leads to decomposition of the Ru complex.<sup>11,12</sup> In the presence of alcohol, as in the catalytic reaction, direct protonation is certainly more favorable. This also applies to the corresponding mechanisms in the mer geometry, where intermolecular protonation by the alcohol competes with intramolecular protonation by the benzylic position. To access intermediate  $F'$ -*fac*, an initial kinetic barrier of 27.0 kcal/mol must be overcome. Nevertheless, this kinetic barrier is much lower than the overall barrier associated with imine reduction by intermediate  $F$ -*mer* (33.7 kcal/mol). Therefore, we postulate that the Ru hydride intermediate  $F'$ -*fac* represents the active reducing species in the catalytic alcohol amination.

**Alcohol Oxidation and Regeneration of the Reducing Species  $F'$ -*fac* and the Catalytic Cycle.** Alcohol oxidation is analogous but reverse in direction to imine reduction and can therefore proceed via the same mechanisms. The potential pathways for the alcohol to aldehyde oxidation and regeneration of the active reducing species  $F'$ -*fac*, namely, an inner-sphere  $\beta$ -hydride elimination mechanism and an outer-sphere concerted hydrogen transfer mechanism, are nearly isoenergetic ( $\Delta\Delta G^\ddagger = 0.6$  kcal/mol; cf. Scheme 7). Therefore, both pathways could be operative under catalytic alcohol amination conditions. Eisenstein and co-workers arrived at a similar conclusion.<sup>34</sup>

### Scheme 7. Inner- and Outer-Sphere Mechanistic Pathways for the Formation of Formaldehyde and the Regeneration of $F'$ -*fac*<sup>a</sup>



The favored pathways for catalyst initiation, imine reduction, and alcohol oxidation sum up to the free energy diagram for the catalytic alcohol amination shown in Figure 3. Once intermediate  $F'$ -*fac* is generated via the high-barrier initiation step (27.0 kcal/mol), it promotes a surprisingly efficient catalytic cycle with an overall kinetic barrier of only 1.8 kcal/mol ( $G_{TS11} - G_{F'-fac} = 1.8$  kcal/mol).

In detail, in the presence of  $NH_3$  as the base, catalyst precursor **B** stoichiometrically oxidizes alcohol to aldehyde and affords Ru hydride complex  $H$ -*mer* via dearomatization of the acridine ligand (Scheme 8). The active reducing species  $F'$ -*fac* is generated from  $H$ -*mer* via a stepwise initiation process with a

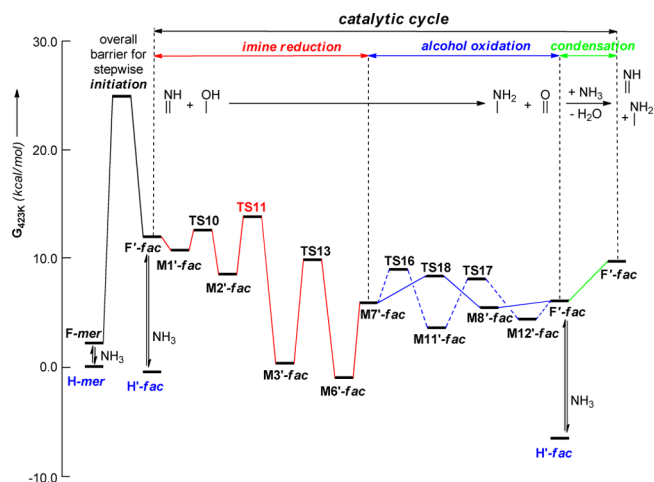
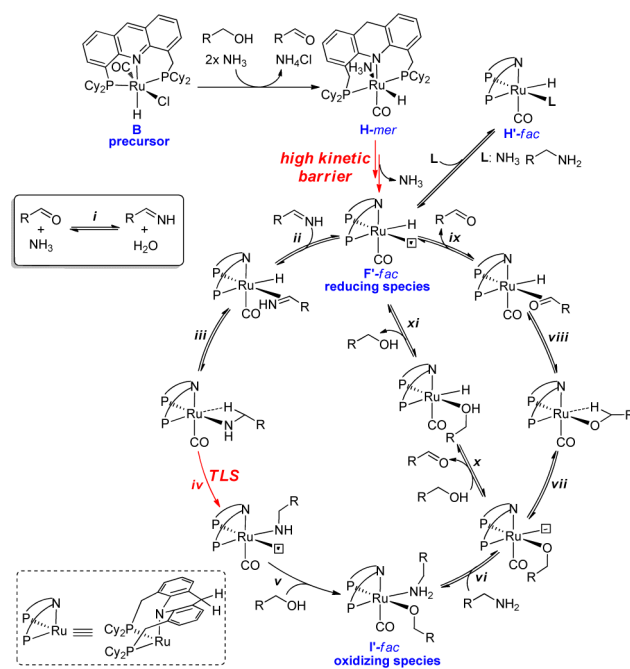


Figure 3. Computed free energy diagram for catalytic methanol amination with  $NH_3$ .

### Scheme 8. Proposed Catalytic Cycle for Alcohol Amination with $NH_3$ Catalyzed by **B**



high kinetic barrier. Complex  $F'$ -*fac* reduces the imine, the product of condensation of the aldehyde with  $NH_3$  (step *i*), via sequential imine coordination and insertion into the Ru–H bond, formation of a pentacoordinated Ru amide intermediate, protonation of the amide moiety by the alcohol, and dissociation of the primary amine product (steps *ii*–*vi*).

The regeneration of the reducing species  $F'$ -*fac* and the formation of the aldehyde can proceed either through inner-sphere  $\beta$ -hydride elimination (steps *vii*–*ix*) or outer-sphere concerted hydrogen transfer (steps *x*–*xi*). The reaction of a Ru– $NH_2$  amide with an alcohol to give a Ru hydride,  $NH_3$ , and an aldehyde is known in the literature.<sup>33</sup> The formation of the pentacoordinate Ru amide (step *iv*) is both the *turnover-limiting* and *selectivity-determining* step of the catalytic cycle ( $G_{TS11} = 13.8$  kcal/mol). This formal  $H_2$ -borrowing redox cycle neither requires a change in the formal oxidation state of ruthenium nor metal–ligand cooperation. This is supported by the

following experimental findings: (1) the complex **H-mer** is the major Ru species in the final reaction mixture of catalytic alcohol amination with  $\text{NH}_3$ ; (2) the primary amine product inhibits the catalytic cycle, as it competes with the imine for the empty coordination site in reducing species **F'-fac**; and (3) complex **H-mer** catalyzes the reductive amination of benzaldehyde with  $\text{NH}_3$  in the absence of alcohol.

**Origin of the Selectivity toward the Primary Amine.** Although a N-substituted imine generated from the condensation of an aldehyde with the primary amine product could also react with the reducing species **F'-fac** to afford the corresponding secondary amine, the overall kinetic barrier of the inner-sphere, alcohol-assisted imine reduction is significantly higher than that of methylamine formation (11.8 vs 1.8 kcal/mol, respectively; Figure 4). Although the stability of **N-**

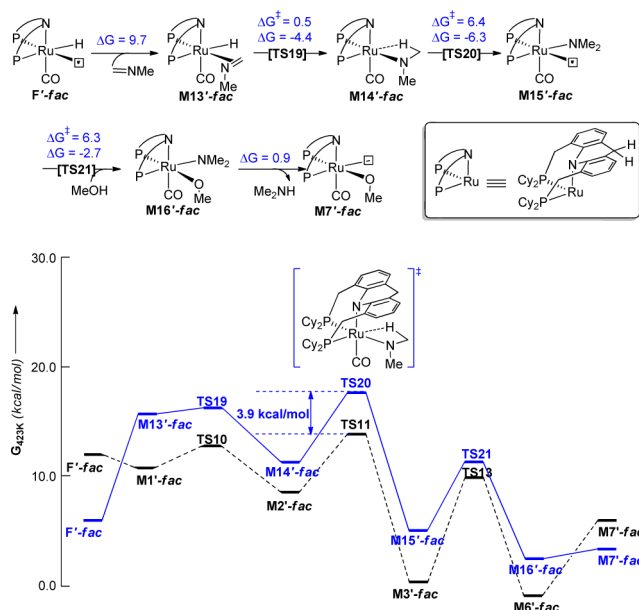


**Figure 4.** Computed free energy diagrams for the formation of dimethylamine (blue) and methylamine (black) via inner-sphere alcohol-assisted imine reduction by **F'-fac**. Calculated energies ( $\Delta G^\ddagger$ ,  $\Delta G$ ) are shown in kcal/mol.

methylimine is higher than that of methanimine by 6.0 kcal/mol,<sup>35</sup> the formation of dimethylamine is still disfavored by 3.9 kcal/mol relative to methylamine. This 3.9 kcal/mol difference in the overall kinetic barrier correlates well with the exceptional primary amine selectivity of **B** observed experimentally. Since the selectivity for primary amine depends directly on the concentrations of the primary and secondary imines, the mechanism explains the observed dependence of the selectivity on the pressure of  $\text{NH}_3$ .

## SUMMARY AND CONCLUSIONS

We have shown that catalyst precursor **B** readily oxidizes primary alcohols to esters in the presence of base at room temperature and is concurrently reduced to the Ru hydride complex **F**. The acridine-based PNP-pincer ligand plays a vital role in this transformation, as one hydrogen atom is stored on the acridine backbone of the anionic dearomatized PNP-pincer ligand framework. Complex **F** is capable of reducing imines to amines at elevated temperature, which is facilitated by an alcohol. In the presence of  $\text{NH}_3$ , **F** rapidly reacts to give the  $\text{NH}_3$ -coordinated Ru hydride complex **H**. Catalytic turnover

can be achieved at elevated temperature with both complex **H** and the in situ-generated imine serving as reducing agents. **H** is also the major Ru species in the reaction mixture of alcohol amination with  $\text{NH}_3$  catalyzed by **B**. Various stereoisomers of the pentacoordinated Ru hydride complex **F** exist as a result of the flexible coordination modes of the anionic dearomatized PNP-pincer ligand. Among the stereoisomers of **F**, **F'-fac** turned out to be the most active species in imine reduction. There is a quite high barrier for the formation of **F'-fac**. However, once generated, intermediate **F'-fac** catalyzes the conversion of the alcohol to the primary amine with a surprisingly low overall barrier for turnover. The turnover- and selectivity-determining step of the catalytic cycle is the reduction of the imine by **F'-fac**, which consists of stepwise formation of the pentacoordinated Ru amide intermediate and subsequent protonation of the Ru amide by an alcohol. The results from this study on structure and function provide an important basis for further insights into the mechanism of similar catalysts.

## ASSOCIATED CONTENT

### Supporting Information

Experimental procedures, additional schemes, characterization data, and details of the calculations. This material is available free of charge via the Internet at <http://pubs.acs.org>. CCDC 913746 (**B**), 913747 (**B'**), 913748 (**E**), 913749 (**F**), and 913750 (**G**) contain the supplementary crystallographic data for this paper. These data can be obtained free of charge from The Cambridge Crystallographic Data Centre via [www.ccdc.cam.ac.uk/data\\_request/cif](http://www.ccdc.cam.ac.uk/data_request/cif).

## AUTHOR INFORMATION

**Corresponding Author**  
ph@oci.uni-heidelberg.de

### Notes

The authors declare no competing financial interest.

## ACKNOWLEDGMENTS

X.Y., P.N.P., M.L., and P.H. work at CaRLa of Heidelberg University, which is cofinanced by Heidelberg University, the state of Baden-Württemberg, and BASF SE. Support from these institutions is gratefully acknowledged.

## REFERENCES

- (1) For reviews of alcohol amination via the  $\text{H}_2$ -borrowing method, see: (a) Bähn, S.; Imm, S.; Neubert, L.; Zhang, M.; Neumann, H.; Beller, M. *ChemCatChem* **2011**, *3*, 1853–1864. (b) Watson, A. J. A.; Williams, J. M. J. *Science* **2010**, *329*, 635–636. (c) Dobereiner, G. E.; Crabtree, R. H. *Chem. Rev.* **2010**, *110*, 681–703. (d) Nixon, T. D.; Whittlesey, M. K.; Williams, J. M. J. *Dalton Trans.* **2009**, 753–762. (e) Guillena, G.; Ramón, D. J.; Yus, M. *Chem. Rev.* **2010**, *110*, 1611–1641.
- (2) For lead references on Ru-catalyzed alcohol amination, see: (a) Hamid, M. H. S. A.; Allen, C. L.; Lamb, G. W.; Maxwell, A. C.; Maytum, H. C.; Watson, A. J. A.; Williams, J. M. J. *J. Am. Chem. Soc.* **2009**, *131*, 1766–1774. (b) Hollmann, D.; Tillack, A.; Michalik, D.; Jackstell, R.; Beller, M. *Chem.—Asian J.* **2007**, *2*, 403–410. For a recent mechanistic study based on the Xantphos ligand, see: (c) Pinggen, D.; Lutz, M.; Vogt, D. *Organometallics* **2014**, DOI: 10.1021/om4011998.
- (3) For lead references on Ir-catalyzed alcohol amination, see: (a) Ohta, H.; Yuyama, Y.; Uozumi, Y.; Yamada, Y. M. A. *Org. Lett.* **2011**, *13*, 3892–3895. (b) Kawahara, R.; Fujita, K.-i.; Yamaguchi, R. J. *Am. Chem. Soc.* **2010**, *132*, 15108–15111. (c) Blank, B.; Madalska, M.;

Kempe, R. *Adv. Synth. Catal.* **2008**, *350*, 749–758. (d) Fujita, K. I.; Fujii, T.; Yamaguchi, R. *Org. Lett.* **2004**, *6*, 3525–3528. (e) Cami-Kobeci, G.; Slatford, P. A.; Whittlesey, M. K.; Williams, J. M. J. *Bioorg. Med. Chem. Lett.* **2005**, *15*, 535–537. (f) Wetzell, A.; Wöckel, S.; Schelwies, M.; Brinks, M. K.; Rominger, F.; Hofmann, P.; Limbach, M. *Org. Lett.* **2013**, *5*, 266–269.

(4) For lead references on Cu-catalyzed alcohol amination, see: (a) Shi, F.; Tse, M. K.; Cui, X.; Gördes, D.; Michalik, D.; Thurow, K.; Deng, Y.; Beller, M. *Angew. Chem., Int. Ed.* **2009**, *48*, 5912–5915. (b) Likhar, P. R.; Arundhati, R.; Kantam, M. L.; Prathima, P. S. *Eur. J. Org. Chem.* **2009**, 5383–5389.

(5) For a lead reference on Fe-catalyzed alcohol amination, see: Martínez, R.; Ramón, D. J.; Yus, M. *Org. Biomol. Chem.* **2009**, *7*, 2176–2181.

(6) For a lead reference on Pd-catalyzed alcohol amination, see: Kwon, M. S.; Kim, S.; Park, S.; Bosco, W.; Chidrala, R. K.; Park, J. J. *Org. Chem.* **2009**, *74*, 2877–2879.

(7) (a) Hayes, K. S. *Appl. Catal., A* **2001**, *221*, 187–195. (b) Klinkenberg, J. L.; Hartwig, J. F. *Angew. Chem., Int. Ed.* **2011**, *50*, 86–95.

(8) Lawrence, S. A. *Amines: Synthesis, Properties and Applications*; Cambridge University Press: Cambridge, U.K., 2005.

(9) For Ru-catalyzed alcohol amination with  $\text{NH}_3$ , see: (a) Gunanathan, C.; Milstein, D. *Angew. Chem., Int. Ed.* **2008**, *47*, 8661–8664. (b) Imm, S.; Bähn, S.; Neubert, L.; Neumann, H.; Beller, M. *Angew. Chem., Int. Ed.* **2010**, *49*, 8126–8129. (c) Pinggen, D.; Müller, C.; Vogt, D. *Angew. Chem., Int. Ed.* **2010**, *49*, 8130–8133. (d) Gunanathan, C.; Milstein, D. *Science* **2013**, *341*, 249–259.

(10) For examples of aromatization–dearomatization in related systems, see: (a) Schwartsburd, L.; Iron, M. A.; Konstantinovski, L.; Diskin-Posner, Y.; Leitus, G.; Shimon, L. J. W.; Milstein, D. *Organometallics* **2010**, *29*, 3817–3827. (b) Khaskin, E.; Iron, M. A.; Shimon, L. J. W.; Zhang, J.; Milstein, D. *J. Am. Chem. Soc.* **2010**, *132*, 8542–8543. (c) Feller, M.; Ben-Ari, E.; Iron, M. A.; Diskin-Posner, Y.; Leitus, G.; Shimon, L. J. W.; Konstantinovski, L.; Milstein, D. *Inorg. Chem.* **2010**, *49*, 1615–1625. (d) van der Vlugt, J. I.; Reek, J. N. H. *Angew. Chem., Int. Ed.* **2009**, *48*, 8832–8846. (e) Ben-Ari, E.; Leitus, G.; Shimon, L. J. W.; Milstein, D. *J. Am. Chem. Soc.* **2006**, *128*, 15390–15391.

(11) Gunanathan, C.; Gnanaprakasam, B.; Iron, M. A.; Shimon, L. J. W.; Milstein, D. *J. Am. Chem. Soc.* **2010**, *132*, 14763–14765.

(12) For a review of the noninnocent behavior of PCP- and PCN-pincer ligands in transition-metal complexes, see: Poverenov, E.; Milstein, D. *Top. Organomet. Chem.* **2013**, *40*, 21–48.

(13) For evidence of metal–ligand cooperation via aromatization–dearomatization in pyridine-based PNP- and PNN-pincer metal complexes, see: (a) Balaraman, E.; Gunanathan, C.; Zhang, J.; Shimon, L. J. W.; Milstein, D. *Nat. Chem.* **2011**, *3*, 609–614. (b) Kohl, S. W.; Weiner, L.; Schwartsburd, L.; Konstantinovski, L.; Shimon, L. J. W.; Ben-David, Y.; Iron, M. A.; Milstein, D. *Science* **2009**, *324*, 74–77.

(14) For computational studies of metal–ligand cooperation via aromatization–dearomatization of pyridine-based PNP- and PNN-pincer metal complexes, see: (a) Yang, X.; Hall, M. B. *J. Am. Chem. Soc.* **2010**, *132*, 120–130. (b) Li, H.; Wang, X.; Huang, F.; Lu, G.; Jiang, J.; Wang, Z.-X. *Organometallics* **2011**, *30*, 5233–5247. (c) Zeng, G.; Li, S. *Inorg. Chem.* **2011**, *50*, 10572–10580. (d) Li, H.; Wen, M.; Wang, Z.-X. *Inorg. Chem.* **2012**, *51*, 5716–5727.

(15) For a review of metal–ligand cooperation via aromatization–dearomatization, see: Gunanathan, C.; Milstein, D. *Acc. Chem. Res.* **2011**, *44*, 588–602.

(16) Gunanathan, C.; Shimon, L. J. W.; Milstein, D. *J. Am. Chem. Soc.* **2009**, *131*, 3146–3147.

(17) A time course study of this redox reaction by in situ  $^1\text{H}$  NMR spectroscopy showed no additional Ru intermediate during this transformation.

(18) See the Supporting Information for  $^1\text{H}$  and  $^2\text{D}$  NMR spectra and corresponding analysis.

(19) Complex **G** can be independently synthesized by exposing a toluene solution of **F** to a  $\text{CO}/\text{H}_2$  atmosphere (rt, <5 min). See the Supporting Information.

(20) Decarbonylation of benzyl alcohol by  $\text{Ru}(\text{Xantphos})(\text{PPh}_3)(\text{CO})\text{H}_2$  led to the formation of  $\text{Ru}(\text{Xantphos})(\text{CO})_2\text{H}_2$ . See: Ledger, A. E. W.; Slatford, P. A.; Lowe, J. P.; Mahon, M. F.; Whittlesey, M. K.; Williams, J. M. J. *Dalton Trans.* **2009**, 716–722.

(21) In contrast to complex **F**, the hexacoordinated complex **H** does not promote the dimerization of aldehyde at room temperature.

(22) (a) Weigend, F.; Ahlrichs, R. *Phys. Chem. Chem. Phys.* **2005**, *7*, 3297–3305. (b) Becke, A. D. *Phys. Rev. A* **1988**, *38*, 3098–3100. (c) Dirac, P. A. M. *Proc. R. Soc. London, Ser. A* **1929**, *123*, 714–733. (d) Slater, J. C. *Phys. Rev.* **1951**, *81*, 385–390. (e) Vosko, S. H.; Wilk, L.; Nusair, M. *Can. J. Phys.* **1980**, *58*, 1200–1211. (f) Perdew, J. P.; Wang, Y. *Phys. Rev. B* **1992**, *45*, 13244–13249. (g) Perdew, J. P. *Phys. Rev. B* **1986**, *33*, 8822–8824.

(23) Andrae, D.; Häussermann, U.; Dolg, M.; Stoll, H.; Preuss, H. *Theor. Chim. Acta* **1990**, *77*, 123–141.

(24) Weigend, F. *Phys. Chem. Chem. Phys.* **2006**, *8*, 1057–1065.

(25) TURBOMOLE version 6.3 2011, a development of the University of Karlsruhe and Forschungszentrum Karlsruhe GmbH, 1989–2007, TURBOMOLE GmbH, since 2007; available from <http://www.turbomole.com>.

(26) In general, gas-phase free energies can be expected to overestimate entropic contributions arising from changes in particle number compared with free energies in solution. Since no mechanistic hypothesis was ruled out solely on the basis of entropic effects, this is not a severe issue.

(27) Zhao, Y.; Truhlar, D. G. *Theor. Chem. Acc.* **2008**, *120*, 215–241.

(28) Schmidt, M. W.; Baldrige, K. K.; Boatz, J. A.; Elbert, S. T.; Gordon, M. S.; Jensen, J. H.; Koseki, S.; Matsunaga, N.; Nguyen, K. A.; Su, S.; Windus, T. L.; Dupuis, M.; Montgomery, J. A., Jr. *J. Comput. Chem.* **1993**, *14*, 1347–1363.

(29) (a) Eckert, F.; Klamt, A. *COSMOtherm*, version C3.0, release 12.01; COSMOlogic GmbH & Co. KG: Leverkusen, Germany, 2012. (b) Eckert, F.; Klamt, A. *AIChE J.* **2002**, *48*, 369–385.

(30) For the crystal structure of the fac-coordinated (dearomatized acridine PNP)Ru(CO)(NH<sub>3</sub>)Cl complex, see ref 11.

(31) Our calculations revealed that in complexes **F** and **H** the *cis*-N,H geometry is generally favored over the *trans*-N,H configuration.

(32) Structural optimization of *F*-*fac* led to activation of the benzylic C–H bond by the Ru center.

(33) The amide moiety in Ru amide complexes is exceptional basic. See: Fulton, J. R.; Sklenak, S.; Bouwkamp, M. W.; Bergman, R. G. *J. Am. Chem. Soc.* **2002**, *124*, 4722–4737.

(34) Nova, A.; Balcells, D.; Schley, N. D.; Dobereiner, G. E.; Crabtree, R. H.; Eisenstein, O. *Organometallics* **2010**, *29*, 6548–6558.

(35) The free energy difference of 6.0 kcal/mol between  $\text{CH}_2=\text{NCH}_3$  and  $\text{CH}_2=\text{NH}$  was obtained by comparing the  $\Delta G$  values for their formations from a mixture of formaldehyde and equal concentrations of  $\text{CH}_3\text{NH}_2$  and  $\text{NH}_3$ . See the Supporting Information.